Valine of the YVDD Motif of Moloney Murine Leukemia Virus Reverse Transcriptase: Role in the Fidelity of DNA Synthesis[†]

Neerja Kaushik,*[,‡] Kajal Chowdhury,§,‖ Virendra N. Pandey,[‡] and Mukund J. Modak*[,‡,§]

Department of Biochemistry and Molecular Biology, Graduate School of Biomedical Sciences and New Jersey Medical School, University of Medicine and Dentistry of New Jersey, 185 South Orange Avenue, Newark, New Jersey 07103

ABSTRACT: The YXDD motif is highly conserved in the reverse transcriptase family. The variable X residue is occupied by valine and methionine in MuLV RT and HIV-1 RT, respectively. Previous studies have shown that Tyr 222, the Y residue of the YXDD motif in MuLV RT, constitutes a major component of the fidelity center of the enzyme [Kaushik, N., Singh, K., Alluru, I., and Modak, M. J. (1999) *Biochemistry* 38, 2617−2627]. In this work, we present evidence that reverse transcriptases containing valine in the "X" position of the YXDD motif generally catalyze DNA synthesis with greater fidelity than those containing methionine or alanine. In the MuLV RT system, the two mutants V223M and V223A exhibited an overall reduced fidelity of DNA synthesis, specifically for RNA-templated reactions. Further analysis revealed that these mutants exhibit a higher efficiency of misinsertion on MS2 RNA than the wild-type enzyme for every mispair tested. However, unlike HIV-1 RT, the insensitivity of the wild-type MuLV RT to all four ddNTPs remained unchanged by mutation of V223 to Met or Ala. A 3D molecular model of the ternary complex of MuLV RT, template primer, and dNTP suggests that Val 223 along with its neighboring Tyr 222 stabilizes the substrate binding pocket via hydrophobic interactions with the dNTP substrate and template-primer.

Reverse transcriptase (RT)[1] is an essential structural component of retroviruses, which is required for the successful propagation of the viral progeny (*1−3*). It is classified as a DNA polymerase since it shares the same general catalytic mechanism and substrate requirements. Using MuLV RT as a model system, we first sought to identify the catalytically important amino acids in this enzyme so that intricacies in the catalytic mechanism of RT could be clarified. We had used chemical modification of RTs using site-specific reagents followed by characterization of the

* Corresponding authors. Phone: 973-972-5515. Fax: 973-972-5594. E-mail: modak@umdnj.edu.

‡ New Jersey Medical School.

§ Graduate School of Biomedical Sciences.

‖ Present address: Department of Biological Chemistry & Molecular Pharmacology, Harvard Medical School, 240 Longwood Ave., Boston, MA 02115.

[1] Abbreviations: HIV-1, human immunodeficiency virus type 1; RT, reverse transcriptase; ddNTPs, dideoxyribonucleotides; MuLV, Moloney murine leukemia virus; WT, wild type; 3D, three dimensional; TP, template-primer; PP$_i$, pyrophosphate; PDB, Protein Data Bank; A, D, M, V, and Y, single-letter codes for the amino acids alanine, aspartate, methionine, valine, and tyrosine, respectively; SDS−PAGE, sodium dodecyl sulfate−polyacrylamide gel electrophoresis; DTT, dithiothreitol; IPTG, isopropyl β-D-thiogalactopyranoside; IMAC, immobilized metal affinity chromatography; PSM, protein solubilizing medium; poly(rA)·(dT)$_{18}$, poly(riboadenylic acid) annealed with (oligodeoxythymidylic acid)$_{18}$; dNTP, deoxyribonucleoside triphosphate; dATP, dGTP, dCTP, and dTTP, nucleoside triphosphates of deoxyadenosine, deoxyguanosine, deoxycytidine, and thymidine, respectively; MS2 RNA, phage MS2 genomic RNA (single stranded); U5-PBS RNA template, HIV-1 genomic RNA template corresponding to the primer binding sequence region; PBS, primer binding site.

modified protein and identification of the sites of modification (*4−7*). Site-directed mutagenesis of desired residues followed by biochemical characterization of the mutant enzyme was subsequently used to examine the importance of some residues in the catalytic process of MuLV RT (*8, 9*). The crystal structures of HIV-1 RT and the Klenow fragment of *Escherichia coli* DNA polymerase I presented an overall arrangement of various domains in these enzymes, thus providing approximation of the 3D outline of the active site pocket in DNA polymerases. Structural comparison and sequence alignment in RTs and DNA polymerases permitted the identification of certain conserved residues in various domains in these enzymes (*10−19*). Using this information as well as that obtained from 3D molecular modeling studies, we identified 10 spatially equivalent residues in the catalytic domain of HIV-1 RT and the Klenow fragment (*20*). Extension of this analysis to MuLV RT revealed the possibility that MuLV RT may also have a similar distribution of conserved residues in its catalytic domain (*9*). However, their functional similarity has not been elucidated. Furthermore, the subunit composition of MuLV RT and that of HIV-1 RT are clearly distinct. MuLV RT is a single-subunit enzyme containing both polymerase and RNase H activities, whereas HIV-1 RT is a two-subunit enzyme and the individual monomeric subunits are inactive (*2, 21−24*). Therefore, it is likely that the participation of the individual residues in the catalysis of DNA synthesis by MuLV RT may be distinct from that observed in HIV-1 RT.

Among the conserved motifs in the catalytic domain of reverse transcriptases, the residues of the YXDD motif in the polymerase active site have been shown to be functionally

important (*13, 15*). Mutation of either one of the two aspartates in this motif, in HIV-1 RT, has been shown to result in complete inactivation of the enzyme protein (*25−31*). Similarly, mutation of one of the two aspartates of the YXDD motif of MuLV RT, Asp 224 to Ala, has also been found to result in a polymerase-deficient phenotype (Chowdhury et al., unpublished results). The X residue of this motif in various RTs has been found to be Met, Val, or Ala (*10−12, 32, 33*). Mutations at Y and M residues of the YMDD motif in HIV-1 RT seems to cause severe to negligible reduction in the enzyme activity (*25, 28, 29, 31, 34−39*). Fidelity of HIV-1 and HIV-2 RTs has been reported to be as much as 10-fold lower than that of MuLV and avian myeloblastosis virus (AMV) RTs (*40−45*). In HIV-1 RT, Met 184 of its YMDD motif has been shown to play a role in the fidelity of DNA synthesis as well as nucleotide analogue resistance since mutation of M184 to V184 was consistently encountered in patients undergoing 3TC therapy (*36−38, 46−50*). To determine if other retroviral polymerases and particularly MuLV RT follow the same general property, we investigated the role of V223 of MuLV RT. In this paper, we report that substitution of valine at position 223 of MuLV RT with methionine or alanine decreases the fidelity of DNA synthesis. However, no compromise in the sensitivity of the mutant enzymes toward different ddNTPs is detected. Molecular modeling of the ternary complex of MuLV RT implicates V223 as a component of the hydrophobic plane, which stabilizes the dNTP binding pocket.

MATERIALS AND METHODS

Cloning of MuLV RT in the Overexpression Vector. The gene coding for MuLV RT was cloned in the overexpression vector pET-28a (Novagen, Madison, WI) as described before (*9*). In brief, a 2016 bp region coding for MuLV RT was amplified by PCR (*51*) from its original plasmid pB6B15.23 (*21*; a kind gift from Dr. S. P. Goff). The amplified fragment was digested with the restriction enzymes *Nde*I and *Eco*RI, which were generated at the 5′ and 3′ end, respectively, during PCR amplification and ligated with the *Nde*I- and *Eco*RI-digested pET-28a vector. The construct pET-28a-MRT contained a hexahistidine sequence and a T7 promoter at the N-terminal region of the MuLV RT coding region (*9*).

Site-Directed Mutagenesis. Mutation of valine at position 223 of MuLV RT to alanine or methionine was carried out by the procedure described by Kunkel et al. (*52*). Briefly, the 847 bp fragment containing the polymerase domain, derived by *Sal*I and *Kpn*I restriction digestion, was cloned in the bacteriophage M13mp19 (Mutagen-M13 in vitro mutagenesis kit, Bio-Rad Laboratories, Hercules, CA) to generate the recombinant plasmid pM13mp19-MRT. The single-stranded deoxyuridine-containing pM13mp19-MRT DNA was used as a template for site-directed mutagenesis using appropriate mutagenesis primers. The mutations were confirmed by dideoxynucleotide sequencing (*53*). The 847 bp fragment containing the desired mutation was subcloned in the pET-28a-MRT expression cassette between the *Kpn*I and *Sal*I sites (*9*).

Expression and Purification of Recombinant MuLV RT. The recombinant plasmid (pET-28a-MRT) containing the coding region for the wild-type and mutant MuLV RT was introduced in *E. coli* BL21 (DE3) for expression. The recombinant wild-type or the mutant enzymes containing the hexahistidine tag were purified by immobilized metal affinity chromatography (IMAC), as described before (*9*). The purity of the enzyme was examined by sodium dodecyl sulfate−polyacrylamide gel electrophoresis (SDS−PAGE) (*54*).

Polymerase Assays. RT activity of the WT and mutant enzymes was determined on three different template-primers, poly (rA)·(dT)$_{18}$, poly (rC)·(dG)$_{18}$, and poly (dC)·(dG)$_{18}$, by monitoring the formation of radioactively labeled nucleic acid product using TCA precipitation assay as described below. The reactions were carried out in a final volume of 100 μL containing 50 mM Tris-HCl, pH 7.8, 1 mM dithiothreitol, 0.01% bovine serum albumin, 300 nM template-primer, 60 mM KCl, 5 mM MgCl$_2$ or 0.5 mM MnCl$_2$, 20 μM [^{3}H] dNTP (1 μCi/assay) complementary to the homopolymeric template, and 25 ng of enzyme. Reactions were initiated by the addition of the respective divalent cation, incubated for 7 min at 37 °C, and terminated by the addition of ice-cold 5% trichloroacetic acid containing 10 mM inorganic pyrophosphate. The acid-precipitated materials were then collected on Whatman GF/B filters and counted for radioactivity in a liquid scintillation counter, as described previously (*9, 55*).

Steady-State Kinetic Analysis of the Polymerase Reaction. Steady-state kinetic constants K_m and k_{cat} for the WT and mutant enzymes were determined using poly(rA)·oligo(dT)$_{18}$ as template-primer and [^{3}H]dTTP as nucleotide substrate essentially as described before (*9, 37, 55, 56*). Template-primers were prepared by mixing 20 μM each of the poly-(rA) template and the oligo(dT)$_{18}$ primer. The reaction mixture (100 μL) contained 50 mM Tris-HCl, pH 7.8, 1 mM DTT, 60 mM KCl, 0.01% BSA, 300 nM template-primer, 5 nM wild-type or mutant enzyme, 0.5 mM MnCl$_2$, and variable amounts of dTTP. The reaction was carried out at 25 °C and terminated by the addition of 5% ice-cold TCA. The acid-precipitable material was collected on GF/B filter paper, and the radioactivity was measured using a liquid scintillation counter. K_m and V_{max} values were determined from Eadie−Hofstee plots of the kinetic data, while k_{cat} was determined from the equation $V_{max} = k_{cat}[E]_{total}$.

Gel Shift Assay. The K_d values for template-primer (DNA−DNA) binding to MuLV RT and its V223 mutant derivatives were carried out by gel mobility shift assay as described by Astatke et al. (*57*) with minor modifications. The ^{32}P-labeled 18mer primer annealed with the 47mer template (Chart 1) was used in this experiment. The labeled template-primer was present at a final concentration of 5 nM in a total reaction volume of 10 μL containing 50 mM Tris-HCl, pH 7.8, 60 mM KCl, 1 mM DTT, 10% glycerol, and enzyme protein ranging from 10 to 1430 nM. The DNA was incubated with increasing concentrations of enzyme for 10 min and loaded onto a 5% polyacrylamide gel in Tris−glycine buffer (25 mM Tris, 162 mM glycine, pH 8.4). The gel was run at 150 V at 4 °C. The radioactive gel bands were counted directly using a Packard Instant Imager. The fraction of the bound DNA was plotted against enzyme concentration, and the K_d value was obtained as the RT concentration at which 50% of the DNA is bound.

Assessment of the Fidelity of DNA Synthesis Using Extension of Primers in the Presence of Three dNTPs. In this assay we used two separate RNA and DNA templates, the U5-PBS RNA, the MS2 RNA, and the 47- and 49mer

Chart 1: Template-Primers Used in Fidelity Determination Assays

U5-PBS RNA template:

3'-CAG GGA CAA GCC CGC GGU GAC GAU CUC UAA AAG GUG UGA CUG AUU UUC CCA GAC UCC CUA GAG AUC AAU GGU CUC AGU GUG UGU UGU CUG CCC GUG UGU GAU GAC UUC UG A GUU CCG UUC GAA AUA AUU CGU CAC CCA AGG GAU CAU CGG UUC UCG AUG GUC CGA GUC UAG A ---------------5' RNA sequence of HIV-1

49 mer:

3'-CAG GGA CAA GCC CGC GGT GAC GAT CTC TAA AAG GTG TGA CTG ATT TTC C -5'

17mer PBS-primer :

5'-GTC CCT GTT CGG GCG CC-3'

18 mer PBS-primer:

5'-GTC CCT GTT CGG GCG CCA-3'

20 mer PBS-primer :

5'-GTC CCT GTT CGG GCG CCA CT-3'

22 mer PBS-primer:

5'-GTC CCT GTT CGG GCG CCA CTG C-3'

47 / 18-mer:

5'-CTT CCA TTC ACA CAC TGC-3'
3'-GAA GGT AAG TGT GTG ACG ATG TCT GAC CTT GTT TTT GTG ACA TTG AG-5'

Chart 2: Sequence of the Template-Primers Used for Kinetic Assessment of Misinsertion Fidelity

MS2 RNA/19C:

5'CGT TAG CCA CTC CGA AGT G -3'
3'GCA AUC GGU GAG GCU UCA CGC AUA UUG CGC GUG CGG CCG CCU GAA ....5'

MS2 RNA/20G:

5'CGT TAG CCA CTC CGA AGT G C-3'
3'GCA AUC GGU GAG GCU UCA CGC AUA UUG CGC GUG CGG CCG CCU GAA ....5'

MS2 RNA/21T:

5'CGT TAG CCA CTC CGA AGT G CG-3'
3'GCA AUC GGU GAG GCU UCA CGC AUA UUG CGC GUG CGG CCG CCU GAA ....5'

MS2 RNA/22A:

5' CGT TAG CCA CTC CGA AGT GCG T -3'
3'GCA AUC GGU GAG GCU UCA CGC AUA UUG CGC GUG CGG CCG CCU GAA....5'

DNA (Charts 1 and 2). U5-PBS HIV-1 RNA containing the primer binding site (PBS) was transcribed from the plasmid pHIV-PBS as described before (*58*). The primers were end labeled with ^{32}P using T4 polynucleotide kinase (New England Biolabs) and [γ-^{32}P]ATP (3000 Ci/mmol, NEN-DuPont), according to the standard protocol (*59*). The desired template was primed with the corresponding ^{32}P-labeled DNA primer and was used to determine the extent of misincorporation and extension in the presence of only three dNTPs as described earlier (*37, 45*). The reaction mixture contained 2.5 nM TP, 50 mM Tris-HCl, pH 7.8, 1 mM DTT, 0.01% BSA, 60 mM KCl, 5 mM MgCl$_2$, and three dNTPs at a final concentration of 1 mM each, in a final volume of 5 μL. Each of the dNTPs used was of the highest purity grade supplied as a 0.1 M solution (Boehringer Mannheim). Equivalent amounts of enzyme activity of the wild type and mutants were used. The reaction mixture was incubated at 25 °C for 30 min and stopped by addition of an equal volume of Sanger's gel loading solution (*53*). Before being loaded, the reaction mixture was heated at 90 °C for 3 min, and a 4.3 μL aliquot was resolved on a denaturing 12% polyacrylamide−urea gel.

Fidelity of DNA Synthesis Using Single Nucleotide Misincorporation Assays. U5-PBS RNA and 49mer U5-PBS DNA were primed with four different 5'-^{32}P-labeled PBS DNA primers of lengths 17, 18, 20, and 22 to provide four different template contexts (Chart 1) to determine the extent

of misincorporation and extension on both RNA and DNA templates in the presence of only a single nucleotide (*60*). Reaction conditions used to determine the 12 possible mismatches and their extension with the WT MuLV RT and its mutants were identical to those used in the presence of three dNTPs with minor modifications. For both RNA and DNA TP, a single dNTP substrate at a final concentration of 500 μM per reaction was used. To determine the fidelity characteristics of the enzyme, equivalent amounts of enzyme activities were used. To analyze the 12 possible mismatches, three different incorrect dNTPs for the first template base were tested independently for each set of template-primer. The reaction products were analyzed by 12% polyacrylamide−urea gel electrophoresis. The products were quantitated by PhosphorImager analysis. The percent misincorporation was determined as the ratio of the wrong nucleotide misincorporated and extended versus the total input labeled primer and plotted as a function of mismatch.

Determination of Kinetic Constants for Misincorporation. Misinsertion kinetics for all mispairs was determined on MS2 RNA using a gel-based steady-state kinetic assay for nucleotide misinsertion (*40, 45, 48, 61, 62*). The primers 19C, 20G, 21T, and 22A (Chart 2) of variable lengths were used to determine misinsertion opposite all four template bases. The nucleotide insertion reaction, in which a 5'-^{32}P-labeled DNA primer is extended by the addition of a dNTP, was performed in the presence of a single dNTP only, using purified, nuclease-free MuLV RT and its two mutant derivatives. Twenty-five picomoles of template and 15 pmol of the desired ^{32}P-labeled DNA primer were annealed in a final volume of 50 μL in a buffer containing 50 mM Tris-HCl, pH 7.8, and 100 mM KCl by heating the mixture to 100 °C for 5 min and allowing it to cool slowly to room temperature. The misinsertion reactions were carried out at varying enzyme concentrations in a buffer containing 300 nM TP (30K Cerenkov counts per lane), 50 mM Tris-HCl, pH 7.8, 1 mM DTT, 0.1% BSA, 60 mM KCl, 5 mM MgCl$_2$, and the respective single dNTP in a final volume of 5 μL. The enzyme concentration varied from 5 to 100 ng per reaction depending on the match or mismatch being determined. The mismatch reactions were carried out at 22 °C at increasing concentrations of dNTP (0.01−10 mM) for an empirically determined reaction time to allow the conversion of about 10−25% of the primer to extended products. Reactions were terminated by the addition of an equal volume of Sanger's gel loading solution (*53*). The products were run on a 12% polyacrylamide−urea gel and quantitated by PhosphorImager analysis using the ImageQuant software. On the basis of the quantitation of unextended and extended primers from each reaction, the initial velocities of product formation were plotted as a function of substrate dNTP concentrations. The initial, linear portion of the curve was employed to obtain the relative V_{max} ($V_{max,rel}$) and K_m values using the Enzyme kinetics program. The $k_{cat,rel}$ was estimated from the ratio of the $V_{max,rel}$/[E]. The catalytic efficiency ($k_{cat,rel}/K_m$ ratios) for each of the 16 possible insertion events, the 12 mispairs and 4 correct base pairs, was then determined as described by Menendez-Arias and colleagues (*63*).

Assay To Determine Sensitivity to ddNTPs. Sensitivity to nucleotide analogue inhibitors 2',3'-dideoxyadenosine 5'-triphosphate (ddATP), 2',3'-dideoxyguanosine 5'-triphosphate (ddGTP), 2',3'-dideoxycytosine 5'-triphosphate (ddCTP), and

Table 1: Polymerase Activity of the Wild-Type MuLV RT and the V223 Mutant Enzymes[a]

enzyme	poly(rA)·(dT)$_{18}$		poly(rC)·(dG)$_{18}$		poly(dC)·(dG)$_{18}$	
	Mg^{2+}	Mn^{2+}	Mg^{2+}	Mn^{2+}	Mg^{2+}	Mn^{2+}
WT	100 (310 ± 5.1)	100 (2507 ± 12.5)	100 (569 ± 7.1)	100 (595 ± 9.0)	100 (273 ± 5.8)	100 (297 ± 12.4)
V223M	124.3 ± 0.7	98.4 ± 0.4	95.3 ± 0.6	106.6 ± 0.7	104.9 ± 2.2	138 ± 8.4
V223A	77.9 ± 1.5	90.7 ± 1.1	89.1 ± 1.6	88.0 ± 5.1	128.9 ± 1.0	135.5 ± 3.1

[a] The polymerase activities of the wild-type MuLV RT and its mutant derivatives were determined on three homopolymeric template-primers in the presence of Mg^{2+} or Mn^{2+} as the divalent metal ions. The values represent a percentage of the WT enzyme activity. Data shown are the mean values ± standard error obtained from two independent experiments. Values shown in parentheses are total picomoles of acid-insoluble dNMP incorporated into primer DNA by 100 ng of the WT enzyme at 37 °C in 10 min.

2′,3′-dideoxythymidine 5′-triphosphate (ddTTP) was examined using heteromeric U5-PBS 49mer DNA and U5-PBS RNA annealed to 5′-^{32}P-labeled 18mer. Reactions were carried out in a total volume of 5 μL in 50 mM Tris-HCl, pH 7.8, 1 mM DTT, 0.01% BSA, 60 mM KCl, 5 mM MgCl$_2$, and 2.5 nM labeled TP at 25 °C for 30 min. A total of 50 ng of the WT MuLV RT, V223M mutant, WT HIV-1 RT, and M184V mutant enzymes was used for each reaction. The ratio of ddNTP to dNTP was 1:2 with the final concentration of each dNTP being 200 μM.

Molecular Modeling Protocol. A prepolymerization ternary complex comprised of the crystal structure of a proteolytic fragment of MuLV RT (*17*), a 4 base pair A-type DNA, ddCTP, and two metal ions was constructed. The components required for the ternary complex were assembled from the crystal structures of various polymerases. The modeling of this ternary complex was based on the crystal structures of DNA-bound HIV-1 RT (*15*) and the ternary complex of T7 DNA polymerase (*19*). The details of the modeling procedure are presented elsewhere (*64*). Briefly, a 4 base pair A-type DNA was constructed using SYBYL molecular modeling software (Tripos Associates Inc., St. Louis, MO) and used to model the ternary complex of HIV-1 RT. The Cα atoms of the palm domain of HIV-1 RT composed of β-strands β6, β9, and β10 and α-helices αE and αF were superimposed on the Cα atoms of the palm domain of MuLV RT (PDB file 1mml) which contains β7, β10, and β11 and α-helices αH and αI. The side chain conformation of the catalytic aspartates and the position of the metal ions in the active site were modeled such that the metals exhibited an octahedral coordination sphere. Modeling of the mutant enzymes of MuLV RT (V223A and V223M) was performed using the molecular modeling software LOOK 2.1 (Molecular Application, Palo Alto, CA).

RESULTS

Construction and Purification of the WT MuLV RT and Its Mutants. The gene construct pET-28a-MRT encoding the wild-type MuLV RT containing hexahistidine at the N-terminal region was used for site-directed mutagenesis as described by Chowdhury et al. (*9*). Two single mutants of the V223 residue were constructed. Induction and purification of the enzymes using a metal affinity IMAC column were carried out as per the standardized protocol described in Materials and Methods. The enzyme was stored in a buffer containing 50 mM Tris-HCl, pH 7.0, 1 mM DTT, 100 mM NaCl, and 50% glycerol. The enzyme preparations were homogeneous as judged by SDS−polyacrylamide gel analysis. The levels of protein expression, yield, solubility, and chromatographic characteristics of the mutant proteins were

Table 2: K_d Values for the WT MuLV RT and the V223 Mutant Derivatives[a]

enzyme	K_d (nM) (47−18mer)
WT	151.7 ± 6.3
V223M	142.8 ± 5.4
V223A	159.2 ± 8.4

[a] The dissociation constant was determined by a gel mobility shift assay using the heteropolymeric 47−18mer template-primer (Chart 1) as described in Materials and Methods.

Table 3: Steady-State Kinetic Constants of WT MuLV RT and the V223M and V223A Mutant Enzymes with Poly(rA)·Oligo(dT)$_{18}$ Template-Primer[a]

enzyme	K_m(dTTP) (μM)	k_{cat} (s^{-1})	k_{cat}/K_m (s^{-1} M^{-1})	ratio (k_{cat}/K_m) mutant/WT
WT	18.7 ± 1.2	2.5	13.4 × 10^4	
V223M	7.4 ± 0.6	1.6	21.6 × 10^4	1.6
V223A	6.7 ± 0.5	1.1	16.4 × 10^4	1.2

[a] The steady-state kinetic parameters for the wild-type MuLV RT and its mutant derivatives were measured with poly(rA)·oligo(dT)$_{18}$ template-primer and Mn^{2+}-dTTP as described in Materials and Methods.

identical to those of the wild-type enzyme, suggesting no significant change in the overall structure of the mutant enzymes.

Polymerase Activity of the Mutant Enzymes on RNA and DNA Templates. The polymerase activity of the wild-type MuLV RT and its mutant derivatives was assessed on homopolymeric poly(rA)·(dT)$_{18}$, poly(rC)·(dG)$_{18}$, and poly-(dC)·(dG)$_{18}$, as described in Materials and Methods, in the presence of Mg^{2+} and Mn^{2+} as the effective divalent cation. As summarized in Table 1, the V223 mutants exhibited 80−140% of the wild-type MuLV RT polymerase activity, depending on the template-primer and the divalent cation. These results suggest that both the methionine and alanine substitutions at V223 in MuLV RT are well tolerated.

Effect of Mutations at Val 223 on K_d DNA. The equilibrium dissociation constant (K_d) for the Val 223 mutants was determined on the DNA−DNA (47−18mer) using gel mobility shift analysis. The equilibrium constant K_d(DNA) was defined as the concentration of enzyme at which half-maximum binding occurred. These results are listed in Table 2 and show nearly identical K_d values for the WT and the two V223 mutants.

Steady-State Kinetic Analyses of the Wild-Type and Mutant Enzymes. Steady-state kinetic analyses were performed for the wild-type and the mutant enzymes using poly(rA)·(dT)$_{18}$ as the template-primer and [^{3}H]dTTP as substrate. As seen in Table 3, a 2−3-fold decrease in the K_m(dTTP) and a corresponding 1.2−1.5-fold decrease in the k_{cat} were observed for the two mutant enzymes. However, the catalytic ef-
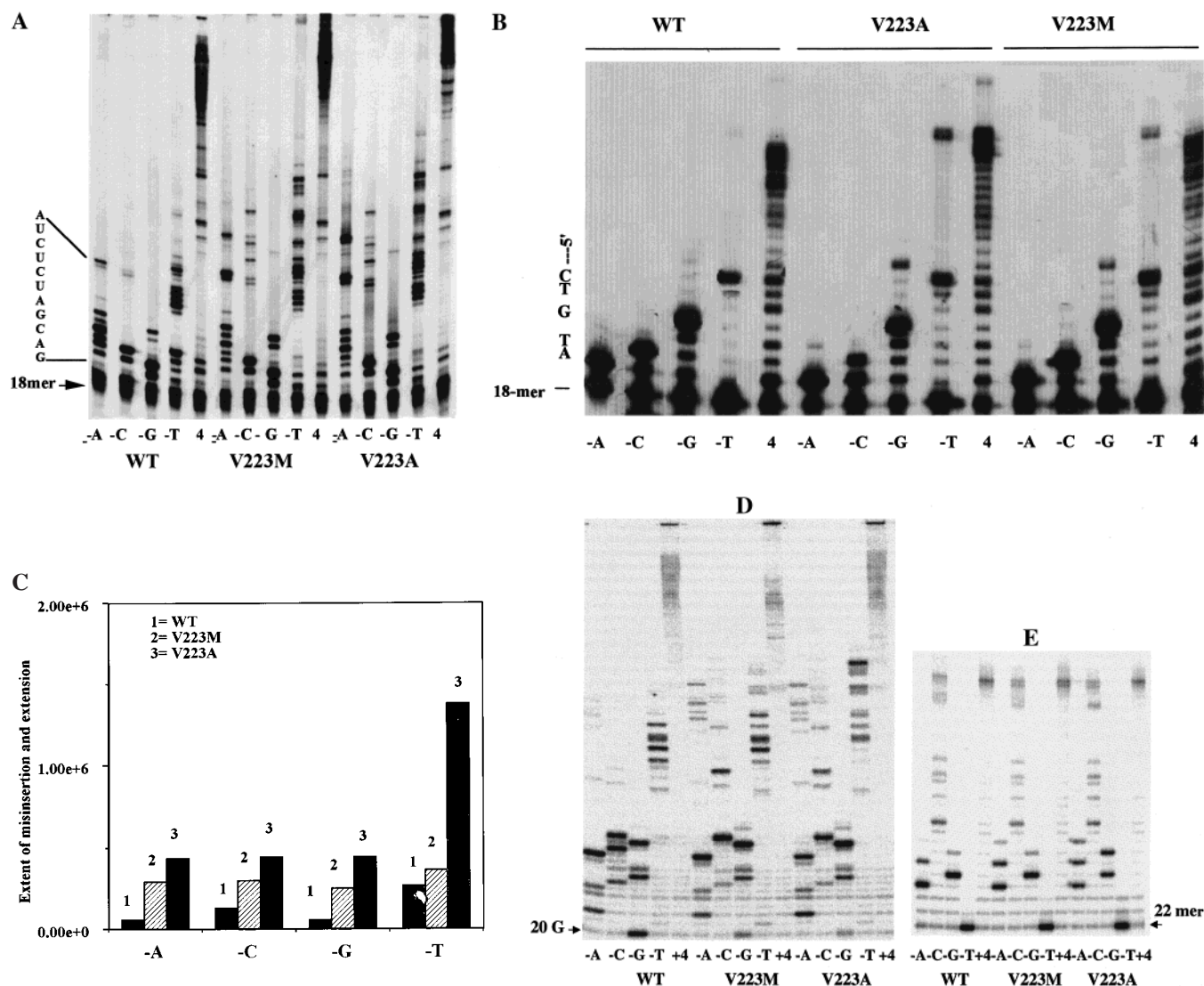
FIGURE 1: Fidelity of DNA synthesis by the wild-type and V223 mutant enzymes on heteropolymeric RNA−DNA and DNA−DNA template-primers in the presence of 3dNTPs. U5-PBS HIV-1 RNA (A), 47mer DNA (C), MS2 RNA (D), and 49mer DNA (E) templates were annealed to their corresponding 5′-^{32}P-labeled primers and used to evaluate the fidelity of wild-type MuLV RT and its mutant derivatives as described in Materials and Methods. Synthesis of misinsertion and its subsequent extension were monitored in the absence of one of the four dNTPs from the reaction mixture. The reaction products were analyzed on a 16% polyacrylamide−urea gel followed by autoradiography. The lanes marked −A, −C, −G, and −T represent the products formed in the absence of the indicated dNTP. The lane marked 4 represents the products synthesized in the presence of all four dNTPs. The template sequence is shown on the left-hand side of the figure. Panel B shows the extent of misinsertion and mispair extension by the wild-type MuLV RT and its mutant derivatives on the U5-PBS HIV-1 RNA template. The intensity of the bands corresponding to the site of misinsertion and subsequent extension shown in panel A were quantitated on a PhosphorImager. The relative band intensities were plotted for each missing dNTP. The sets marked −A, −C, −G, and −T represent misinsertion and mispair extension events for the corresponding missing nucleotide.

ficiency (k_{cat}/K_m) of both enzymes (V223A, V223M) was similar to that of the wild-type enzyme. These results also suggest that the decrease in K_m of the mutant enzymes may be a reflection of a decrease in k_{cat}. The RNase H activity of these mutants was not altered, as judged by gel analysis of the RNase H cleavage products (data not shown). These results indicate that Val at position 223 of MuLV RT may not be directly involved in the binding and turnover of the dNTP substrates and the subsequent catalytic steps of DNA synthesis. However, the V223 equivalent residue in HIV-1 RT has been implicated in fidelity of DNA synthesis (*37, 38*). Therefore, we examined the properties of V223 and its mutant derivatives in this aspect.

Misincorporation and Mispair Extension Fidelity in the Presence of Three Nucleotides. To examine the effect of Val

to Met substitution at position 223 on the fidelity of DNA synthesis by MuLV RT, misinsertion and extension of the misincorporated nucleotides were evaluated under conditions where one of the four dNTPs was omitted from the reaction mixture (*37, 45*). The 47- and 49mer DNA, U5-PBS HIV-1 RNA, and MS2 RNA templates primed with the complementary 5′-^{32}P-labeled DNA primers were used as template-primers as described previously (*64*). Results shown in Figure 1 are representative of the pattern of misincorporation and its extension against template bases T/U, G, C, and A. The lanes marked −A, −C, −G, and −T represent reaction products obtained in the absence of the corresponding nucleotide. Generally, the absence of any one of the four dNTPs results in the accumulation of product, prior to the site of the missing nucleotide. The appearance of products

beyond the site of the missing nucleotide indicates incorporation of a noncomplementary nucleotide. As seen in Figure 1A,D, the wild-type enzyme exhibits the highest fidelity on both of the RNA templates, followed by the V223M and V223A mutants, respectively. However, with all enzymes, the extent of misincorporation varied depending on the template base encountered. Thus, on the U5-PBS HIV-1 RNA template, the V223M mutant enzyme exhibited an increase in the extent of error by 2−6-fold, while the V223A mutant was in the range of 4−8-fold (Figure 1B). On DNA templates, a somewhat mixed fidelity pattern was obtained. On a 47−18mer template-primer the WT enzyme exhibited relatively higher fidelity than the V223 mutants (Figure 1C). Surprisingly, on a 49mer DNA template containing the same sequence as the U5-PBS HIV-1 RNA template, no significant difference in the fidelity pattern, between the wild-type and V223 mutant enzymes, was observed (Figure 1E). These observations suggest that misincorporation and mispair extension are dependent on the nature of the template as well as the template base encountered.

Nucleotide Misincorporations by the Wild-Type and Mutant Enzymes in the Presence of a Single Nucleotide. To further investigate the 12 possible nucleotide misincorporations and mispair extension opposite the 4 template bases, we used the U5-PBS RNA and 49mer U5-PBS DNA templates annealed with primers of varying lengths such that four different template contexts are provided (Chart 1). With each template-primer, four individual reactions were carried out with each of the four single nucleotide substrates. A control reaction in the presence of all four dNTPs was also carried out under similar conditions. The concentration of the WT and mutant enzymes was adjusted to provide nearly equivalent enzyme activity. The individual products of misinsertion and mispair extension were quantitated by PhosphorImager analysis as a ratio of the wrong nucleotide misincorporated and extended versus the total amount of primer present in the reaction. The results are shown in Figure 2. The overall pattern for fidelity of DNA synthesis on the RNA template in the presence of a single nucleotide showed a trend similar to that seen in the presence of three dNTP substrates. The WT enzyme exhibited the highest fidelity of DNA synthesis, followed by the V223M and V223A mutants. However, despite the changes in the absolute extent of infidelity, both the WT enzyme and the mutants exhibited the maximal mispairs constituted by the G·T, T·G and C·T, T·C, followed by the C·A, G·A mispairs (Figure 2B). Most interestingly, of the 12 possible mismatches, 3 opposite each template base, the least favored mismatch by all enzymes corresponded to the homologous mispairs, i.e., A·A, T·T, C·C, and G·G (Figure 2B).

Surprisingly, very little misincorporation and extension were seen with the 49mer U5-PBS DNA template-primer of identical sequence to that of U5-PBS RNA and with both WT MuLV RT and its mutant derivatives. Thus, unlike HIV-1 RT, which exhibits mispair formation and its extension on both RNA and DNA templates, MuLV RT exhibits a significantly marked increase in relative misincorporation frequency on RNA templates only. Our results are in general agreement with those reported earlier for WT MuLV RT (*43, 65*).

Kinetics of Misinsertion. The nucleotide misincorporation assay described above provides a qualitative indication of

the type/nature and extent of misincorporation and its extension by WT MuLV RT and its mutant derivatives in the presence of saturating concentrations of a single nucleotide on the U5-PBS HIV 1 RNA template. To quantitatively estimate the misinsertion efficiency (f_{ins}) by V223M and V223A for all 12 mispairs and to determine if the nature of mismatch was influenced by the sequence context of the template-primer, we carried out steady-state kinetic analysis using the MS2 RNA as a template. For this determination, the labeled primers 19C, 20G, 21T, and 22A providing dCTP, dGTP, dTTP, and dATP as the first incoming nucleotide, respectively, were annealed to the MS2 RNA. Reactions were carried out at 22 °C. The concentrations of the enzyme were adjusted such that, for all the mismatches, conversion of about 10−25% of the primer to extended products occurred in 5−25 min of incubation. The individual product bands on the gel were quantitated on a PhosphorImager using the ImageQuant program (Molecular Dynamics). The kinetic parameters for misinsertion on MS2 RNA by the wild-type MuLV RT and the V223 mutants and the estimate of misinsertion efficiency are summarized in Tables 4 and 5. As seen from the steady-state kinetic parameters for the single correct and incorrect nucleotide insertion (Table 4), the k_{cat} values for the corresponding pairs and mispairs generated by the wild-type MuLV RT and the two V223 mutants exhibited no significant alteration except in the case of C·T, G·T, and T·T mispairs, where some differences were observed. However, the K_m values for the correct as well as the incorrect dNTP substrate exhibited significant differences. The WT enzyme consistently exhibited a higher K_m value for every mispair generated compared to the mutants. This was in marked contrast to the relatively lower K_m values seen with the wild-type enzyme for the correct base pairs. The overall catalytic efficiency for the correct nucleotide incorporation by the WT MuLV RT and its V223 mutant derivatives ranged from 3.34×10^7 to 1.21×10^9, whereas for the incorrect nucleotide this range was from about 20 to 4500. As is evident from the f_{ins} values (Table 5), the wild-type MuLV RT displayed a higher fidelity of insertion than the two mutants of V223. Between the two mutants, V223M exhibited an overall higher fidelity than the V223A mutant. The range of misinsertions for the WT enzyme varied from 1.2×10^{-6} to 8.0×10^{-8}. In case of the V223M and V223A mutants this range varied from 3.2×10^{-4} to 7.4×10^{-7} and from 2.2×10^{-4} to 7.8×10^{-6}, respectively. Although both mutants displayed a consistently decreased fidelity of insertion than the wild-type enzyme for all mispairs generated, they exhibited a much higher increase in the misinsertion efficiency in the formation of two mispairs i.e., A·G and T·C (Table 5). Additionally, the V223A mutant also displayed a greater insertion infidelity for the C·A, C·C, G·G, and G·T mispairs. Among various mispairs, both the mutants displayed relatively decreased misinsertion efficiency for the C·T and T·T mispairs.

Sensitivity of the Wild-Type and Mutant Enzymes toward Dideoxynucleoside Triphosphates. An interesting property of certain mutants of HIV-1 RT is reflected in the observation that mutations which increased the fidelity of the enzyme also made them less sensitive to ddNTP inhibitors. For example, M184V and E89G mutants of HIV-1 RT appeared to better discriminate against ddNTPs versus dNTPs (*48, 50*) compared to the wild-type enzyme. It was therefore interest-
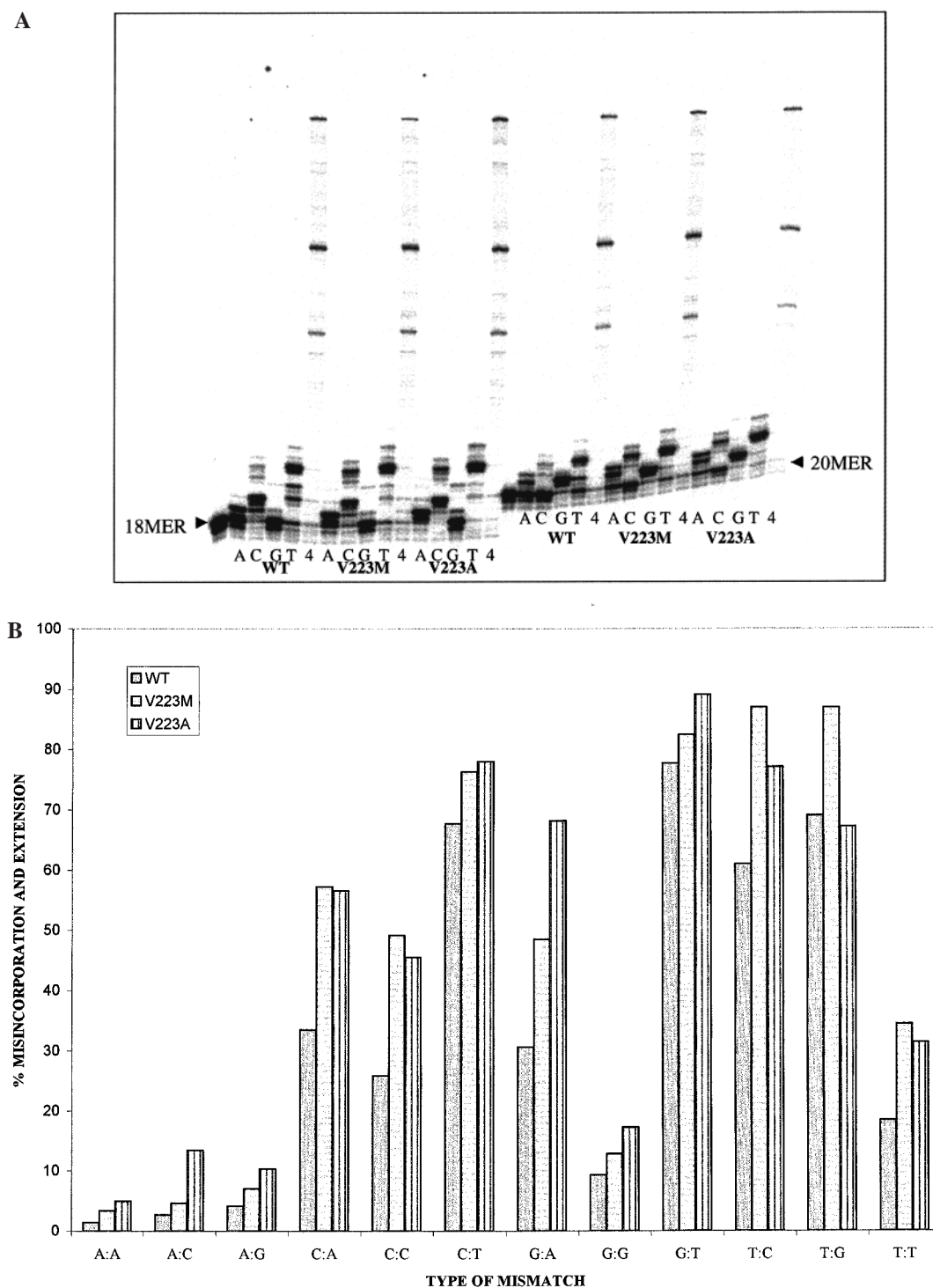
FIGURE 2: Graphic representation of the extent of misinsertion and mispair extension catalyzed by the wild-type MuLV RT and its V223 and V223A derivatives in the presence of a single dNTP with different template context. (A) The ability of the enzymes to generate and extend mispairs in the presence of a single dNTP was assessed on U5-PBS RNA primed with 5′-³²P-labeled 17-, 18-, 20-, or 22mer (Chart 1). The enzymes were incubated at 25 °C for 30 min with 2 nM labeled template-primer in a 5 μL reaction mixture. Experiments were carried out with each of the above-mentioned primers in the presence of a single indicated dNTP to determine all of the individual mismatches. A control lane with all four dNTPs was also included for comparison. Results obtained with 18- and 20mer PBS primers are shown as a representative for this set of experiments. Lanes marked A, C, G, and T represent reactions carried out in the presence of dATP, dCTP, dGTP, and dTTP, respectively. Lane 4 represents the products synthesized in the presence of all four dNTPs. **(B)** Fidelity assays were carried out on a U5-PBS RNA primed with one of the four different primers having A, C, G, or T as the first template nucleotide in the presence of a single dNTP substrate as described in panel A. Band intensities were scanned on a PhosphorImager and quantitated. The percentage of both misincorporation and mispair extension with each enzyme was calculated and plotted for each mismatch as described in Materials and Methods.

ing to examine the status of the WT MuLV RT in regard to its sensitivity toward four dideoxynucleotide chain terminators and then to examine if mutations in MuLV RT, which alter the fidelity of the enzyme, would now exhibit change in the sensitivity to nucleotide analogue inhibitors. Since, the HIV-1 RT containing equivalent mutation was readily

Table 4: Kinetic Parameters for Misinsertion on MS2 RNA by WT MuLV RT and V223 Mutants

base pair[a]	$k_{cat,rel}$[b] (% min^{-1})			K_m[b] (μM)			k_{cat}/K_m (% min^{-1} M^{-1})		
	WT	V223M	V223A	WT	V223M	V223A	WT	V223M	V223A
AT	123.8 ± 2.6	102.2 ± 4.7	99.5 ± 5.3	0.102 ± 0.032	0.765 ± 0.22	0.483 ± 0.16	1.21 × 10^9	1.34 × 10^8	2.06 × 10^8
AA	0.6 ± 0.04	0.6 ± 0.05	0.58 ± 0.04	405 ± 132	335 ± 131	243 ± 80	1.48 × 10^3	1.79 × 10^3	2.38 × 10^3
AC	0.55 ± 0.02	0.53 ± 0.02	0.53 ± 0.02	255 ± 50	191 ± 33	183 ± 41	2.16 × 10^3	2.77 × 10^3	2.89 × 10^3
AG	0.54 ± 0.001	0.52 ± 0.002	0.54 ± 0.001	32 ± 3	12 ± 2	12 ± 5	1.69 × 10^4	4.33 × 10^4	4.5 × 10^4
CG	87.5 ± 1.8	106.7 ± 2.7	80.7 ± 6.2	0.22 ± 0.04	0.849 ± 0.175	1.92 ± 0.79	3.97 × 10^8	1.25 × 10^8	4.2 × 10^7
CA	0.12 ± 0.001	0.14 ± 0.02	0.18 ± 0.03	198 ± 83	81 ± 6.1	67 ± 5.6	6.06 × 10^2	1.73 × 10^3	2.68 × 10^3
CC	0.02 ± 0.001	0.02 ± 0.001	0.03 ± 0.001	471 ± 148	134 ± 90	113 ± 55	4.24 × 10	1.49 × 10^2	2.65 × 10^2
CT	0.29 ± 0.01	0.22 ± 0.02	0.13 ± 0.01	517 ± 106	430 ± 200	400 ± 129	5.6 × 10^2	5.12 × 10^2	3.25 × 10^2
GC	44.5 ± 0.3	40.0 ± 0.9	48.7 ± 0.9	0.064 ± 0.017	0.288 ± 0.07	0.383 ± 0.05	6.95 × 10^8	1.39 × 10^8	1.27 × 10^8
GA	0.03 ± 0.001	0.05 ± 0.001	0.04 ± 0.001	536 ± 112	490 ± 24	404 ± 47	5.59 × 10	1.02 × 10^2	0.99 × 10
GG	0.06 ± 0.001	0.05 ± 0.001	0.05 ± 0.001	433 ± 74	198 ± 14	120 ± 13	1.38 × 10^2	2.53 × 10^2	4.16 × 10^2
GT	0.48 ± 0.06	0.6 ± 0.02	0.65 ± 0.01	477 ± 36	319 ± 62	237 ± 20	1.00 × 10^3	1.88 × 10^3	2.74 × 10^3
TA	45.3 ± 0.2	57.8 ± 1.2	45.7 ± 2.9	0.507 ± 0.121	1.73 ± 0.17	0.92 ± 0.34	8.93 × 10^7	3.34 × 10^7	4.97 × 10^7
TC	0.04 ± 0.001	0.05 ± 0.001	0.04 ± 0.001	675 ± 40	57 ± 21	16 ± 4	5.92 × 10	8.77 × 10^2	2.5 × 10^3
TG	0.01 ± 0.001	0.02 ± 0.001	0.02 ± 0.001	541 ± 36	284 ± 26	162 ± 75	1.84 × 10	7.04 × 10	1.23 × 10^2
TT	0.52 ± 0.03	0.51 ± 0.07	0.62 ± 0.04	695 ± 122	465 ± 39	572 ± 145	7.48 × 10^2	1.1 × 10^3	1.08 × 10^3

[a] Base pairs are shown with the template base first. [b] Both $k_{cat,rel}$ and K_m are relative values determined by using the Enzyme kinetics program. The standard deviations presented are derived from two independent measurements.

Table 5: Misinsertion Efficiency on MS2 RNA by the WT MuLV RT and V223 Mutants

mis-pair	f_{ins}[a]			fold increase in misinsertion efficiency	
	WT	V223M	V223A	V223M	V223A
AA	1.22 × 10^{-6}	1.34 × 10^{-5}	1.15 × 10^{-5}	10.9	9.4
AC	1.78 × 10^{-6}	2.08 × 10^{-5}	1.41 × 10^{-5}	11.7	7.9
AG	1.39 × 10^{-5}	3.24 × 10^{-4}	2.18 × 10^{-4}	23.3	15.7
CA	1.52 × 10^{-6}	1.37 × 10^{-5}	6.39 × 10^{-5}	9	42
CC	1.07 × 10^{-7}	1.19 × 10^{-6}	6.32 × 10^{-6}	11.1	59.1
CT	1.41 × 10^{-6}	4.09 × 10^{-6}	7.73 × 10^{-6}	2.9	5.5
GA	8.04 × 10^{-8}	7.35 × 10^{-7}	7.79 × 10^{-8}	9.1	0.9
GG	1.99 × 10^{-7}	1.82 × 10^{-6}	3.28 × 10^{-6}	9.2	16.5
GT	1.45 × 10^{-6}	1.35 × 10^{-5}	2.16 × 10^{-5}	9.3	14.9
TC	6.33 × 10^{-7}	2.62 × 10^{-5}	5.03 × 10^{-5}	41.4	79.5
TG	2.07 × 10^{-7}	2.11 × 10^{-6}	2.48 × 10^{-6}	10.2	12
TT	8.37 × 10^{-6}	3.28 × 10^{-5}	2.18 × 10^{-5}	3.9	2.6

[a] Evaluated from $k_{cat,rel}/K_m$ ratios of incorrect versus correct nucleotides in Table 4 as described in refs 48, 62, and 63.

available in the laboratory (*37*), we also included the M184V mutant and the WT HIV-1 RT in this study. The experiment to assess sensitivity to the individual dideoxynucleoside triphosphate was carried out using U5-PBS HIV-1 RNA template primed with ^{32}P-labeled 17mer PBS DNA primer as described in Materials and Methods. The identical pattern of products synthesized by all three enzyme species of MuLV RT in both the presence and absence of the ddNTP inhibitors shows that neither the wild-type V223 MuLV RT nor the V223M or V223A mutants exhibited any sensitivity toward anyone of the dideoxynucleotide inhibitors tested (data not shown). Similarly, no alteration in the sensitivity of MuLV RT mutants was noted when DNA was replaced for RNA as a template in an identical experiment (data not shown). In contrast to MuLV RT or its mutants, the HIV-1 RT and its M184V mutant indeed exhibited sensitivity to all four ddNTPs to different extents. As noted before, some reduction in the sensitivity to some dideoxynucleotides was also confirmed with the M184V mutant (*36*–*38*, *46*–*50*). These results clearly demonstrate that MuLV RT differs from HIV-1 RT, implying some fine differences in the contribution

of the X residue to the substrate binding pocket in the individual RT.

DISCUSSION

Val 223 of MuLV RT is a variable member (the X residue) of the highly conserved YXDD motif in the reverse transcriptase family (*10*–*12*, *32*, *33*). Investigation of its role in the catalytic process, i.e., template-primer or substrate dNTP binding (Tables 2 and 3) by comparative analyses of the properties of its two mutant phenotypes, indicated no direct role for this residue. This is inspite of the fact that its neighboring residues, on either side, are catalytically essential (*25*–*31*). However, our studies indicate that Val at this position plays an important role in the fidelity of DNA synthesis of the enzyme, since its mutation to either Met or Ala results in relatively more error-prone enzyme (Figures 1 and 2). In this regard, comparison of its properties to HIV-1 RT may be appropriate. HIV-1 RT is known to be the most error-prone enzyme among various RTs tested (*40*–*45*). Furthermore, the presence of M at position X in the YXDD motif of HIV-1 RT has been identified as one of the major residues conferring the "error-prone" character. In vitro replacement of Met 184 (in the YXDD motif) with Val resulted in a decreased error rate (*36*–*38*, *50*). Considering the similarity of overall results of V to M mutation in MuLV RT and that of Met to Val mutation in HIV-1 RT, the nature of participation of Val 223 in the stabilization of the primer terminus is likely to be similar to that proposed for HIV-1 RT (*37*).

Our results on the steady-state kinetic parameters of DNA synthesis for the wild-type MuLV RT and V223A and V223M mutant derivatives indicate that both of the mutant enzymes have slightly lower K_m values for dTTP as well as a slight decrease in k_{cat} (Table 3). Similarly, the examination of K_d(DNA) of the WT or mutant enzyme indicated little change. Therefore, the effects that we note in the misinsertion properties may not be directly related to the alterations in the affinity for substrates. To qualitatively test the fidelity of DNA synthesis, we used two RNA–DNA and DNA–DNA templates of known sequence and allowed the exten-

sion of primer by the wild-type or the mutant enzyme in the presence of only three nucleotides (Figure 1). Our results indicate that the wild-type MuLV RT exhibited the highest fidelity of DNA synthesis on both of the RNA templates examined, followed by the V223M and V223A mutants in decreasing order. A somewhat mixed fidelity pattern was obtained on DNA templates. The WT enzyme exhibited relatively higher fidelity than the V223 mutants on a 47−18mer template-primer (Figure 1C). However, on a 49mer DNA template having the same sequence as the U5-PBS HIV-1 RNA template, no significant difference in the fidelity pattern was observed (Figure 1E). These observations suggest that misincorporation and mispair extension are dependent on the nature of the template as well as the template base encountered. Examination of the extent of misincorporation and its extension on the U5-PBS HIV-1 RNA template showed that all enzymes displayed the maximum percent error for the G·T, T·G, T·C, and C·T mispairs (Figure 2B). Nonetheless, for most mismatches the V223A mutant exhibited the highest percent error, followed by the V223M mutant and the WT enzyme. In contrast, on a 49mer DNA template of the same sequence, no significant difference in the misincorporation and extension could be seen between the WT and mutant enzymes (results not shown).

To gain better insight into the mechanism by which Val at 223 position influences the fidelity of MuLV RT, we carried out a detailed investigation of the kinetic parameters governing nucleotide misinsertion. For this, we used the MS2 RNA, since we found that this RNA serves as a better template for kinetic examination of misincorporation compared to the U5-PBS HIV-1 RNA. One reason may be attributed to the difference in the secondary structures of the two RNAs. This also allowed us to compare if the nature and extent of mismatch formation differed between the two RNA templates. Our steady-state kinetic analysis for single incorrect nucleotide incorporation revealed an increase in K_m for all the mispairs generated by the WT enzyme as well as its two mutant derivatives. The catalytic efficiency for incorrect nucleotide incorporation showed a decrease by 4 to 7 orders of magnitude. This decrease was relatively more pronounced for the WT enzyme compared to the two mutant derivatives. We would, however, like to caution that the steady-state kinetic parameters for single nucleotide misinsertion do not provide the precise mechanistic step responsible for the observed changes in the kinetic constants. The rate-limiting step governing the correct and incorrect nucleotide incorporation by the WT MuLV RT versus its V223 mutant derivatives can be more reliably obtained by carrying out a pre-steady-state kinetic analysis for a single dNTP turnover as pointed out by Johnson and colleagues (66). In the case of HIV-1 RT, a pre-steady-state kinetic analysis by Kati et al. (67) has indeed shown significantly higher K_d values for the incorrect dNTP. The insertional fidelity (f_{ins}) values indicated that the wild-type MuLV RT displayed a higher fidelity of insertion than the two mutants of V223 (Table 5). Comparison between the two mutants indicated that V223M exhibited somewhat higher fidelity than the V223A MuLV RT (Tables 4 and 5). Irrespective of the mispair generated, the wild-type enzyme exhibited a decreased misinsertion efficiency for all mispairs other than the V223 mutants. However, the increase in misinsertion efficiency by both of the mutants was significantly more
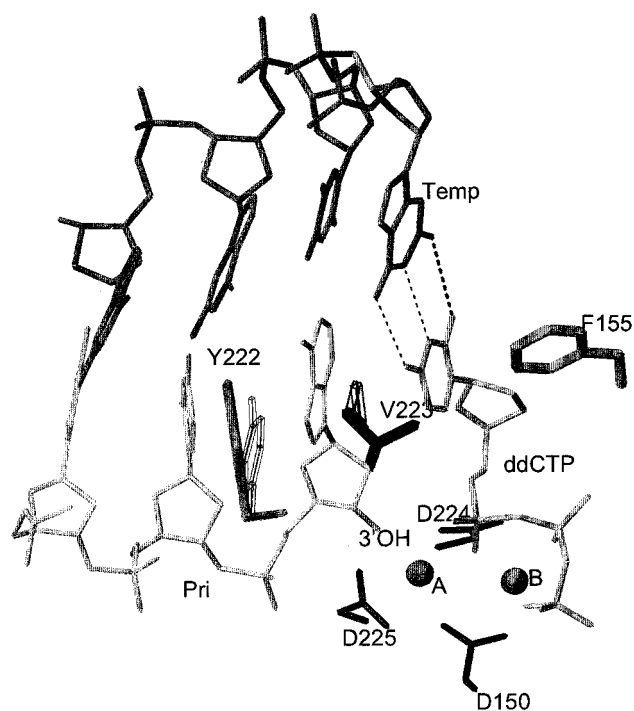

FIGURE 3: 3D molecular model of the catalytic core of MuLV RT complexed with modeled DNA and ddNTP. A prepolymerization ternary complex model of MuLV RT shows the position of the YVDD motif residues. This model contains a part of the template-primer, ddCTP, two metal ions (A and B), and side chains of the residues of the YVDD motif of MuLV RT. The side chain of D150 has been included to complete the catalytic carboxylate triad, whereas F155 is the part of the hydrophobic plane that stabilizes the sugar moiety of dNTP. Although we considered F199 as a part of the hydrophobic plane, the side chain for this residue is not shown in this figure for clarity. The dotted lines between the template base and the incoming dNTP (represented by ddCTP) show the Watson−Crick hydrogen-bonding pattern. The side chains of the wild-type enzyme are shown as solid sticks whereas those for V223M or V223A are in outline format (next to the wild-type position). This figure shows that the mutation of V223 to M or A also slightly alters the side chain orientation of Y222.

pronounced for the A·G, C·A, and T·C mispairs (Table 5). In contrast, the least misinsertion efficiency was observed for the C·T and T·T mispairs.

Studies on HIV-1 RT have suggested a functional correlation between sensitivity to nucleotide analogues and fidelity of DNA synthesis (37, 38, 48, 49, 68). Several drug-resistant variants of HIV-1 RT, e.g., M184L, M184V, E89G, and L74V, exhibit increased fidelity in vitro relative to the WT enzyme (37, 38, 48, 49, 68). In contrast, the V223M and V223A mutants of MuLV RTs display marked resistance to all four dideoxynucleotides in a fashion similar to that of the wild-type enzyme (data not shown). This suggests that the mechanism for discrimination against a nucleotide analogue and an incorrectly base-paired nucleotide may be different. Preliminary results have shown that Q190 of MuLV RT may be one of the sites that contributes to ddNTP discrimination (Singh et al., manuscript in preparation). The residue in MuLV RT responsible for the discrimination between ddNTP and dNTP is yet to be identified.

The prepolymerization ternary complex model of MuLV RT containing ddCTP, template-primer, and two metal ions is shown in Figure 3. The side chains contributing to the hydrophobic plane (Y222, F155, and F199) along with the

side chains of V223 in the active site region of MuLV RT have been shown in this figure. The modeled ternary complex shows that V223 is within interacting distance with the sugar moiety of the primer terminus. Thus, the function of this residue in MuLV RT may be related to the stabilization of the primer terminus. A similar molecular interaction of M184 in HIV-1 RT was also inferred from the prepolymerase complex model of HIV-1 RT (*37*). Our biochemical data on V223 show that the mutation of this residue by Met or Ala does not alter the activity of the enzyme; however, the mutant enzymes appear more error prone than the wild-type enzyme. Therefore, V223 of MuLV RT may be considered as a residue, which directly or indirectly influences the fidelity of the enzyme. It has been noted recently that the mutation of the neighboring Y222 to F222 in MuLV RT confers significantly improved fidelity characteristics on MuLV RT (*64*). These results suggest that multiple residues may contribute to the process of fidelity of DNA synthesis. Our molecular modeling shows that replacement of V223 by A or M changes the position of the side chain of Y222. Therefore, the change in the fidelity of MuLV RT may also be an indirect effect of the altered interactions of Y222. On the basis of these results we conclude that the nature of the X residue of the YXDD motif of the reverse transcriptase contributes to the fidelity of DNA synthesis. Reverse transcriptases containing valine at this position have higher insertion fidelity than those containing methionine or alanine. However, this residue does not appear to influence the ddNTP insensitivity in MuLV RT. We would also like to point out that while this paper was under revision, a report from Pathak and colleagues describing a novel in vivo assay to identify the structural determinants in MuLV RT important for fidelity has appeared (*69*). These authors have reached the same general conclusion that Val 223 to Met 223 mutation results in a more error-prone phenotype.

ACKNOWLEDGMENT

REFERENCES

1. Baltimore, D. (1970) *Nature 226*, 1209−1211.
2. Skalka, A. M., and Goff, S. P. (1993) *Reverse transcriptase*, CSHL Press, Plainview, NY.
3. Temin, H. M., and Mizutani, S. (1970) *Nature 226*, 1211−1213.
4. Basu, A., Nanduri, V. B., Gerard G. F., and Modak, M. J. (1988) *J. Biol. Chem. 263*, 1648−1653.
5. Basu, S., Basu, A., and Modak, M. J. (1993) *Biochem. J. 296*, 577−583.
6. Nanduri, V. B., and Modak, M. J. (1990) *Biochemistry 29*, 5258−5264.
7. Reddy, G., Nanduri, V. B., Basu, A., and Modak, M. J. (1991) *Biochemistry 30*, 8195−8201.
8. Basu, A., Basu, S., and Modak, M. J. (1990) *J. Biol. Chem. 265*, 17162−17166.
9. Chowdhury, K., Pandey, V. N., Kaushik, N., and Modak, M. J. (1996) *Biochemistry 35*, 16610−16620.
10. Delarue, M., Poch, O., Tordo, N., Moras, D., and Argos, P. (1990) *Protein Eng. 3*, 461−467.
11. Johnson, M. S., McClure, M. A., Feng, D. F., Gray, J., and Doolittle, R. F. (1986) *Proc. Natl. Acad. Sci. U.S.A. 83*, 7648−7652.
12. Xiong, Y., and Eickbush, T. H. (1990) *EMBO J. 9*, 3353−3362.
13. Kohlstaedt, L. A., Wang, J., Friedman, J. M., Rice, P. A., and Steitz, T. A. (1992) *Science 256*, 1783−1790.
14. Steitz, T. A., Smerdon, S., Jager, J., and Joyce, C. M. (1994) *Science 266*, 2022−2025.
15. Jacobo-Molina, A., Ding, J., Nanni, R. G., Clark, A. D., Lu, X., Tantillo, C., Williams, R. L., Kamer, G., Ferris, A. L., Clark, P., Hizi, A., Hughes, S. H., and Arnold, E. (1993) *Proc. Natl. Acad. Sci. U.S.A. 90*, 6320−6324.
16. Pelletier, H., Sawaya, M. R., Kumar, A., Wilson, S. H., and Kraut, J. (1994) *Science 264*, 1891−1903.
17. Georgiadis, M. M., Jassen, S. M., Ogata, C. M., Telesnitsky, A., Goff, S. P., and Hendrickson, W. A. (1995) *Structure 3*, 879−892.
18. Tantillo, C., Ding, J., Jacobo-Molina, A., Nanni, R. G., Boyer, P. L., Hughes, S. H., Pauwels, R., Andries, K., Janssen, P. A. J., and Arnold, E. (1994) *J. Mol. Biol. 243*, 369−387.
19. Doublie, S., Tabor, S., Long, A. M., Richardson, C. C., and Ellenberger, T. (1998) *Nature 391*, 251−258.
20. Yadav, P. N. S., Yadav, J. S., Arnold, E., and Modak, M. J. (1994) *J. Biol. Chem. 269*, 716−720.
21. Roth, M. J., Tanese, N., and Goff, S. P. (1985) *J. Biol. Chem. 260*, 9326−9335.
22. Verma, I. M. (1977) *Biochim. Biophys. Acta 473*, 1−38.
23. Lightfoote, M. M., Coligan, J. E., Folks, T. M., Fauci, A. S., Martin, M. A., and Venkatesan, S. (1986) *J. Virol. 60*, 771−775.
24. Dimarzo-Veronese, F., Copeland, T. D., DeVico, A. L., Rahman, R., Oroszlan, S., Gallo, R. C., and Sarangadharan, M. G. (1986) *Science 231*, 1289−1291.
25. Boyer, P. L., Ferris, A. L., and Hughes, S. H. (1992) *J. Virol. 66*, 1031−1039.
26. Hostomsky, Z., Hostomska, Z., Fu, T. B., and Taylor, J. (1992) *J. Virol. 66*, 3179−3182.
27. Kaushik, N., Rege, N., Yadav, P. N. S., Sarafianos, S. G., Modak, M. J., and Pandey, V. N. (1996) *Biochemistry 35*, 11536−11546.
28. Larder, B. A., Purifoy, D. J. M., Powell, K. L., and Darby, G. (1987) *Nature 327*, 716−717.
29. Larder, B. A., Kemp, S. D., and Purifoy, D. J. M. (1989) *Proc. Natl. Acad. Sci. U.S.A. 86*, 4803−4807.
30. LeGrice, S. F. J., Nass, T., Wohlgensinger, B., and Schatz, O. (1991) *EMBO J. 10*, 3905−3911.
31. Lowe, D. M., Parmar, V. S., Kemp, D., and Larder, B. A. (1991) *FEBS Lett. 282*, 231−234.
32. Doolittle, R. F., Feng, D. F., Johnson, M. S., and McClure, M. A. (1989) *Q. Rev. Biol. 64*, 1−30.
33. Poch, O., Sauvaget, I., Delarue, M., and Tordo, N. (1989) *EMBO J. 8*, 3867−3874.
34. Boyer, P. L., and Hughes, S. P. (1995) *Antimicrob. Agents Chemother. 39*, 1624−1628.
35. Chao, S. F., Chan, V. L., Juranka, P., Kaplan, A. H., Swanstrom, R., and Hutchison, C. A., III (1995) *Nucleic Acids Res. 23*, 803−810.
36. Larder, B. A., Kemp, S. D., and Harrigan, P. R. (1995) *Science 269*, 696−699.
37. Pandey, V. N., Kaushik, N., Rege, N., Sarafianos, S. G., Yadav, P. N. S., and Modak, M. J. (1996) *Biochemistry 35*, 2168−2179.
38. Wainberg, M. A., Drosopoulos, W. C., Salomon, H., Hsu, M., Brokow, G., Parniak, M. A., Gu, Z., Song, Q., Manne, J., Islam, S., Castriota, G., and Prasad, V. R. (1996) *Science 271*, 1282−1285.

39. Harris, D., Yadav, P. N. S., and Pandey, V. N. (1998) *Biochemistry 37*, 9630−9640.

40. Preston, B. D., Poiesz, B. J., and Loeb, L. A. (1988) *Science 242*, 1168−1171.

41. Roberts, J. D., Bebenek, K., and Kunkel, T. A. (1988) *Science 242*, 1171−1173.

42. Bakhanashvilli, M., and Hizi, A. (1992) *FEBS Lett. 306*, 151−156.

43. Bakhanashvilli, M., and Hizi, A. (1992) *Biochemistry 31*, 9393−9398.

44. Ji, J., and Loeb, L. A. (1992) *Biochemistry 31*, 954−958.

45. Yu, H., and Goodman, M. F. (1992) *J. Biol. Chem. 267*, 10888−10896.

46. Gu, Z., Gao, Q., Li, X., Parniak, M. A., and Wainberg, M. A. (1992) *J. Virol. 66*, 7128−7135.

47. Wakefield, J. K., Jablonski, S. A., and Morrow, C. D. (1992) *J. Virol. 66*, 1031−1039.

48. Drosopoulos, W. C., and Prasad, V. R. (1996) *J. Virol. 70*, 4834−4838.

49. Bakhanashvilli, M., Orna, A., and Hizi, A. (1996) *FEBS Lett. 391*, 257−262.

50. Hsu, M., Inouye, P., Rezende, L., Richard, N., Li, Z., Prasad, V. R., and Wainberg, M. A. (1997) *Nucleic Acids Res. 25*, 4532−4536.

51. Saiki, R. K., Scharf, S., Faloona, F., Mullis, K., Horn, G. T., Erlich, H. A., and Arnheim, N. (1985) *Science 230*, 1350−1354.

52. Kunkel, T. A., Roberts, J. D., and Zakour, R. A (1987) *Methods Enzymol. 154*, 367−382.

53. Sanger, F., Nicklen, S., and Coulson, A. R. (1977) *Proc. Natl. Acad. Sci. U.S.A. 74*, 5463−5467.

54. Laemmli, U. K. (1970) *Nature 227*, 680−685.

55. Kaushik, N., Pandey, V. N., and Modak, M. J. (1996) *Biochemistry 35*, 7256−7266.

56. Majumdar, C., Abbotts, J., Broder, S., and Wilson, S. H. (1988) *J. Biol. Chem. 263*, 15657−15665.

57. Astatke, M., Grindley, N. D. F., and Joyce, C. M. (1995) *J. Biol. Chem. 270*, 1945−1954.

58. Arts, E. J., Li, X., Gu, Z., Kleiman, L., Parniak, M., and Wainberg, M. A. (1994) *J. Biol. Chem. 269*, 14672−14680.

59. Ausubel, F. M., Brent, R., Kingston, R. E., Moore, D. D., Seidman, J. S., Smith, J. A., and Struhl, K. (1987) *Current Protocols in Molecular Biology*, Greene Publishing Associates and Wiley-Interscience, John Wiley & Sons, New York.

60. Perrino, F. W., Preston, B. D., Sandell, L. L., and Loeb L. A. (1989) *Proc. Natl. Acad. Sci. U.S.A. 86*, 8343−8347.

61. Ricchetti, M., and Buc, H. (1990) *EMBO J. 9*, 1583−1593.

62. Boosalis, M. S., Petruska, J., and Goodman, M. F. (1987) *J. Biol. Chem. 262*, 14689−14696.

63. Martin-Hernandez, A. M., Gutierrez-Rivas, M., Domingo, E., and Menendez-Arias, L. (1997) *Nucleic Acids Res. 25*, 1383−1389.

64. Kaushik, N., Singh, K., Alluru, I., and Modak, M. J. (1999) *Biochemistry 38*, 2017−2021.

65. Bakhanashvilli, M., and Hizi, A. (1993) *FEBS Lett. 319*, 201−205.

66. Patel, S. S., Wong, I., and Johnson, K. A. (1991) *Biochemistry 30*, 511−525.

67. Kati, W. M., and Johnson, K. A. (1992) *J. Biol. Chem. 267*, 25988−25997.

68. Rubinek, T., Bakhanashvili, M., Taube, R., Avidan, O., and Hizi, A. (1997) *Eur. J. Biochem. 247*, 238−247.

69. Halvas, E. K., Svarovskaia, E. S., and Pathak, V. K. (2000) *J. Virol. 74*, 312−319.